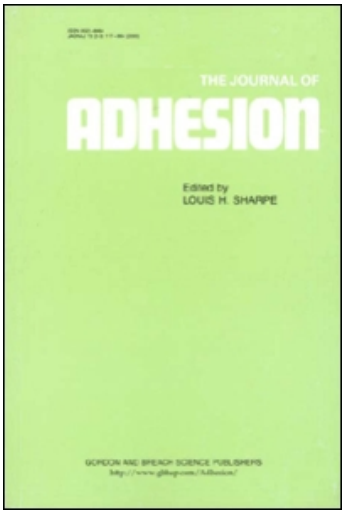

The Journal of Adhesion
Publication details, including instructions for authors and subscription information:
http://www.informaworld.com/smpp/title~content=t713453635

Adhesion and Hydrolytic Stability of the Interface Between High-Modulus Polyethylene Fibers and Acrylic Resins

Z. -F. Li[a]; A. T. Dibenedetto[a]; J. Jancar[a]; J. Goldberg[b]
[a] Institute of Materials Science, University of Connecticut, Storrs, CT, USA [b] School of Dentistry, University of Connecticut Health Center, Farmington, CT, USA

To cite this Article Li, Z. -F. , Dibenedetto, A. T. , Jancar, J. and Goldberg, J.(1995) 'Adhesion and Hydrolytic Stability of the Interface Between High-Modulus Polyethylene Fibers and Acrylic Resins', The Journal of Adhesion, 50: 4, 249 — 264
To link to this Article: DOI: 10.1080/00218469508014556
URL: http://dx.doi.org/10.1080/00218469508014556

J. Adhesion, 1995, Vol. 50, pp. 249–264
Reprints available directly from the publisher
Photocopying permitted by license only

Adhesion and Hydrolytic Stability of the Interface Between High-Modulus Polyethylene Fibers and Acrylic Resins

Z.-F.Li, A. T. DIBENEDETTO and J. JANCAR

Institute of Materials Science, University of Connecticut, Storrs, CT 06269, USA

J. GOLDBERG

School of Dentistry, University of Connecticut Health Center, Farmington, CT 06030, USA

(Received October 27, 1994; in final form February 15, 1995)

The effects of oxyen plasma treatment on the surface chemistry of Spectra 1000® high modulus polyethylene fibers and on the mechanical properties of fiber-reinforced composites of the fibers in a Bis-GMA based acrylic resin have been studied. X-ray photoelectron spectroscopy and diffuse reflectance FTIR spectroscopy have been used to show that the majority of oxygen on the fiber surface exists mostly in the form of ether and/or epoxy linkages, with carbonyl-, carboxylic- and ester-containing compounds accounting for less than 10 percent of the total. While the untreated and plasma-treated fibers have similar chemical compositions, the surfaces of the plasma-treated fibers are more polar and the oxygen is chemically bonded instead of being merely physisorbed. The interfacial shear strength between the fibers and the acrylic resin is increased by a factor of 2.3 by the plasma treatment indicating the presence of a weak boundary layer on the surface of the untreated fibers. The hydrolytic stability of the composite interfaces was investigated for fibers sized with several Bis-GMA-based adhesives. Maximum stability was attained by sizing with Bis-GMA containing a peroxide catalyst or an amine accelerator. The flexural properties of composites utilizing plasma-treated and untreated fibers were compared in three-point bending. The ultimate bending loads for composites using treated fibers were much higher than those for composites with untreated fibers, but only a fraction of that for glass or Kevlar®-reinforced materials.

KEY WORDS: adhesion between polyethylene fibers and acrylic resin; interfaces in composites; spectroscopic analysis of interfaces; hydrolytic stability of interfaces; high modulus polyethylene fibers; mechanical properties of SPECTRA fiber reinforced composites.

INTRODUCTION

High modulus polyethylene fibers are produced by gel spinning[1,2] with strengths and Young's moduli of the order of 2–5 GPa and 100–200 GPa, respectively,[3,4] comparable with carbon, glass and aramid fibers but with a greater fracture resistance. Their use in fiber-reinforced composite applications is limited by low melting temperature, low compressive strength, high creep rate and poor adhesion to polymeric matrices. They are used with other fibers, however, to produce hybrid composites with improved fracture toughness.[5]

Acrylic resins reinforced with particulate or fibrous inorganic materials are commonly used in dental and orthopedic applications. While such materials have high

stiffness, they often have poor resistance to impact and crack propagation. Small amounts of high modulus polyethylene fibers have been added to the acrylic matrices in an attempt to increase their toughness and, thereby, increase their potential for use in dental applications.[6-13] Poor adhesion of the polyethylene fiber to the acrylic matrices, however, leads to a significant reduction in the flexural strength and stiffness of the composite material. Fiber surface treatments by corona and plasma discharges and acid oxidation have been used to improve the adhesion.[14-19] Although oxygen plasma treatments have been employed commercially for this purpose, the surface modification of the fibers has not been fully described. In this work, we characterize the fiber surface chemistry before and after an oxygen plasma treatment and examine its effects on interfacial adhesion and mechanical properties of the fiber reinforced composites. X-ray photoelectron spectroscopy (XPS) and diffuse reflectance Fourier transform infra-red spectroscopy (DRIFT) are used to examine the chemical composition of the surface. The effect on hydrolytic stability of the fiber/matrix interface of sizing the fibers with various acrylic resin adhesives based on 2,2 bis(2-hydroxy-3-methacryloxy propoxy) phenyl propane (Bis-GMA) is also investigated.

EXPERIMENTAL

Materials Preparation

High modulus polyethylene fibers, Spectra 1000, were supplied by Allied Fibers Company. The oxygen-plasma-treated Spectra 1000 fibers were provided by Plasma Sciences Inc.. The plasma treatment was carried out on a standard PS1010 continuous treatment device with an RF generator operating at a power of 300 Watts and a frequency of 13.56 MHz. The vacuum pressure in the plasma treatment chamber was 0.5 torr. The residence time of fiber in the chamber was one minute. The system is described in Reference 15. To study the stability of the fibers' surface chemical composition and to free them of surface contaminants, the fibers were extracted with methanol for twenty-four hours in a Soxhlet extractor. The extracted components in the methanol were not identified.

An acrylic adhesive was prepared from a mixture of 70 pph of bisphenol-A-glycidyl methacrylate (Bis-GMA), 30 pph of triethylene glycol dimethacrylate (TEGDMA), 0.75 pph of benzoyl peroxide catalyst (BPO) and 0.1 pph of 2,4,6, tritertiarybutyl phenol antioxidant (TTBP). After thorough mixing, dry argon gas was bubbled through to purge any dissolved oxygen and the mixture was used as the matrix for the fiber-reinforced composites (FRC). The bulk polymerization was carried out isothermally under argon gas at a temperature of 80°C for 2.5 hours, followed by another 2 hours at 120°C.

The Spectra 1000 fibers were also sized with various Bis-GMA-based adhesive mixtures. Five sizing solutions were prepared using dichloromethane as the solvent. They are as follows: 2wt% 70pphBis-GMA/30pph TEGDMA; 0.02M Bis-GMA; 0.04M Bis-GMA; 0.04 M Bis-GMA/2.5%BPO catalyst; 0.04M Bis-GMA/2.5% n-n dimethylaniline (DMA) accelerator. Fiber bundles about 20 cm long were immersed in an excess of solution for 5 minutes and then dried under argon at 80°C for 2 hours. In addition, the polyethylene fibers were treated with $SiCl_4$ using a procedure suggested

by Gomez *et al.*,[20,21] in an attempt to bond the Bis-GMA chemically to a chlorinated siloxane surface. Plasma-treated fibers were dried at 120°C for 4 hours and stored in a desiccator. A 250 ml Erlenmeyer flask was dried at 200°C overnight in a vacuum oven. After cooling down the oven to 120°C, a fiber bundle of 20 cm length was put into the flask under an argon gas purge and the flask was sealed with a rubber septum. An excessive amount of freshly-distilled n-heptane solvent, which was dried with calcium hydride for over a week, was transferred to the flask using a double-tipped needle. The volume of solvent was determined by weighing the flask before and after solvent transfer. Then $SiCl_4$ in a sufficient amount to form a concentration of 0.05 M was transferred to the flask using a syringe. The reaction was carried on for 48 hours at room temperature. The solution was then drained using a double-tipped needle, and dry heptane solvent was transferred to the flask to wash the fiber bundle. After draining the solvent, the fiber bundle with the flask was placed in an oven purged with argon. Immediately after removing the septum, vacuum was turned on to evaporate the heptane solvent. The temperature of the oven was then raised to 80°C and the fibers were dried in vacuum for 2 hours. After drying, the fiber bundle was transferred to another dry flask sealed with a septum. A solution of 0.01 M Bis-GMA in dichloromethane was prepared. Anhydrous dichloromethane containing less than 50 ppm water was further dried with calcium hydride. Since each Bis-GMA molecule contains two hydroxyl groups, we expected the Bis-GMA to react with the chlorines on the $SiCl_4$-treated fibers. The grafting reaction was carried out at 80°C for 24 hours. The fiber bundle was then removed from the solution and dried at 60°C in an oven for 2 hours. The procedure was not optimized to promote maximum coverage or properties.

Pre-preg fiber composite tapes were filament wound as described elsewhere.[22] A fiber tow was passed through a bath of uncured resin matrix and then through a roller couple. A pressure was applied to the fibers to squeeze out excess resin and insure wetting. The fiber volume fraction was controlled by adjusting the pressure applied to the tow. The impregnated tow was wound on a mandrel and B-staged for one hour at 80°C under argon. To prevent dripping of the resin, the mandrel was frequently rotated in the oven. After B-staging, the pre-preg was taken out of the oven and cooled down to room temperature. At this point, the pre-preg, although stiff enough to handle, was still tacky. It was then cut into sheets of 150 mm long by 50 mm wide. The thickness of pre-preg sheets was approximately 0.2 mm. Five plies of pre-preg were laid up in an mold for compression molding using a Wabash model hydraulic hot press. The press was first heated to 100°C, then the aluminum mold was placed between the lower and upper platens. A load of 2.5 tons, producing a pressure of approximately 3 MPa, was gradually applied to the laminate. The composite was cured under pressure for 30 minutes. After releasing the composite from the aluminum mold, it was further cured at 120°C for another 2 hours. The molded composite has a uniform thickness and smooth surface.

Surface Characterization

Elemental and chemical compositions of the polyethylene fiber surfaces were determined using a Perkin Elmer model 5300 XPS spectrometer. The XPS spectra were obtained using a monochromatic Al Kα x-ray which was generated at an anode voltage

of 15 kV and anode power of 550 Watts. The acquisition time for collecting the peak signals was two hours or a peak-to-noise ratio of 200, whichever came first. An electron flood gun was used to neutralize the static charges on the fiber surfaces. Fiber bundles 2 cm long were held on a steel sample holder, which was placed in the XPS ultra-high vacuum chamber operating at a pressure of the order of 10^{-9} torr. A high-resolution spectrum was then collected for each identified element over a range of 20 eV around its peak binding energy with a pass energy of 8.95 eV and a spot size 0.3 mm in diameter. The oxygen-to-carbon element ratio was calculated using the following equation:

$$O/C = I_o\sigma_c / I_c\sigma_o \quad (1)$$

where I_o and I_c are the peak areas and σ_0 and σ_c are the photoionization cross-sections for O_{1s} and C_{1s}, respectively.

The two peak profiles were deconvoluted to analyze for chemical bonding ratios. The deconvolution process yielded the percentage of C—C, C—O, C=O and O—C=O groups. Further deconvolution of C—O into C—OH and C—O—C, in order to determine the concentration of —OH containing compounds on the fiber surface, is of special importance since the hydroxyl groups are used to react with $SiCl_4$ and, subsequently, to graft Bis-GMA to the fiber surface. In order to quantify the concentration of hydroxyl groups on the fiber surface, the hydroxyl groups were tagged by reacting them with trifluoro acetic anhydride.[23] Four fiber bundles about 2 cm long were placed in a 20 ml vial and dried at 110°C for about 12 hours. The vial was then sealed with a rubber septum, cooled to room temperature and charged with about 50 µl of trifluoro acetic anhydride. After 10 minutes, the fibers were removed from the vial. To remove physisorbed trifluoro acetic anhydride and acids, the fibers were heated at 90°C in an oven for 30 minutes.

The diffuse reflectance infra-red (DRIFT) spectra were collected using a Nicolet 60SX FT-IR system with an MCT detector.[24] The fibers were first ground with KBr powders to form a felt, and then placed in the sample holder. By subtracting the KBr reference spectrum from the fiber signal, interference from CO_2 and moisture in the sample chamber and possible contamination on the reflection mirrors in the optical path were eliminated. A total of 1024 scans were collected for each fiber sample.

Surface topography of fibers with various treatments were examined using an Amray scanning electron microscope. An accelerating voltage of 15 KV was used throughout the study. In order to prevent electron beam damage, the fibers were well-coated with a gold palladium alloy and the photography was accomplished as soon as possible after selecting an area for imaging.

The fiber surface free energies were determined from the contact angles of glycerol and a liquid epoxy resin (DER331 from Dow Chemical) spreading on the fibers using the scheme described by Carroll[25] and Wagner.[26] The contact angle of a liquid droplet on a single fiber was determined by measuring the height and length of the droplet. The polar and dispersion components of fiber surface free energy were calculated using the following equation:

$$\cos\theta = 2[(\gamma_s^d \gamma_l^d)^{1/2} + (\gamma_s^p \gamma_l^p)^{1/2}]/\gamma_l - 1 \quad (2)$$

where γ refers to the surface free energy, its subscripts s and l refer to the solid substrate and the contacting liquid, respectively, and superscripts d and p refer to the dispersion

and polar components, $\gamma_s = \gamma_s^d + \gamma_s^p$ and $\gamma_l = \gamma_l^d + \gamma_l^p$. The γ_l, γ_l^d, and γ_l^p for glycerol are 64, 34, 30 mJ/m^2, respectively.[27] The surface energies of epoxy and Bis-GMA were obtained by measuring the contact angles of the epoxy on a low density polyethylene sheet and a Plexiglas PMMA sheet. The literature values of the surface free energies of polyethylene, γ_s, γ_s^d, and γ_s^p, are 35.3, 35.3, 0 mJ/m^2 respectively, and 41.1, 29.6, 11.6 mJ/m^2, respectively, for PMMA.[28] The contact angle and surface energies for epoxy and Bis-GMA are shown in Table I.

Single-fiber pull-out specimens were prepared using a technique developed by Li and Grubb.[29] A fiber is embedded normal to the thickness direction of a resin, without a contact meniscus at the entrance of fiber to the resin. Figure 1 is a schematic of the fiber pull-out test. The tests were carried out on an MTS model 810 servovalve controlled tensile testing machine with a two-pound (0.91 kg) load cell. The free fiber length between a capstan clamp and the resin sheet was 50 mm. The opening between the two plates of the micro-vise was kept constant by a 50 μm thick sheet of paper. A typical load *vs* displacement curve obtained during pull-out is linear to a peak load, F_p, corresponding to complete interfacial debonding. When the fiber slips through the resin sheet after complete debonding, the load decreases to the dynamic frictional force, F_{fr}. The average interfacial shear strength, τ_a, and average dynamic frictional stress, τ_{fr}, were calculated using the following equations:

$$\tau_a = F_p/2r_f l_e = \sigma_p r_f/2l_e \tag{3}$$

$$\tau_{fr} = F_{fr}/2r_f l_e = \sigma_{fr} r_f/2l_e \tag{4}$$

TABLE I
Contact Angle and Surface Free Energy of Bis-GMA and Epoxy

	Contact Angle, Degree		Surface Free Energy, mJ/m^2		
Resin	Polyethylene	PMMA	γ_l	γ_l^d	γ_l^p
Epoxy	49.2 (± 5.3)	21.7 (± 0.1)	43.3	36.6	6.7
Bis-GMA	42.0 (± 0.87)	12.9 (± 2.7)	42.1	27.9	14.2

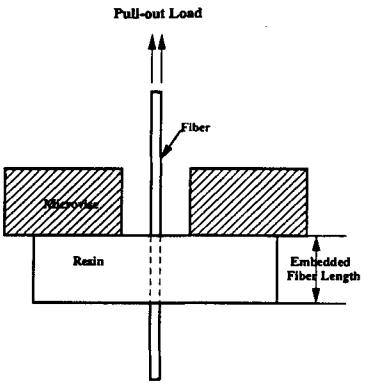

FIGURE 1 Schematic Illustration of Single Fiber Pull-out Test.

where l_e is the embedded fiber length, or the thickness of the resin sheet, σ_p is peak pull-out stress, σ_{fr} is the fiber stress due to the dynamic frictional resistance, and r_f is the fiber radius. The embedded fiber length was normally 1.0 mm. At least ten specimens were tested for each condition. The cross-sections of the polyethylene fibers were slightly elliptical and have a significant variation in cross-sectional area along the fiber. To have a reasonably accurate measure of the average diameter of the embedded part, the fiber was pulled a little further out from the resin after the pull-out test. The original embedded length can be easily distinguished by its topography, and its point of entry is marked by bending or shear damage. The fiber diameter was then measured with a microscope. To test hydrolytic stability, the specimens were immersed in pre-distilled boiling water for 24 hours and then tested at room temperature while still wet.

Since the average interfacial shear strength, τ_a, depends strongly on the embedded fiber length, l_e, the embedded length was varied from 0.15 mm to 2.5 mm to obtain a relationship between τ_a and l_e, for comparison of our results with those of other workers who used different embedded lengths.

Three-point bending tests were carried out at a span-to-depth ratio of 60, using standard procedures of ASTM D796. Five-ply laminate strips 0.25 mm wide by 150 mm long were cut from the compression-molded plates. Laminates of Kevlar-and E-glass-fiber-reinforced composites were prepared in a similar manner for comparison with the polyethylene fiber composites. A minimum of 5 specimens were tested for each composite material. The initial bending modulus was calculated using the following equation:

$$M_b = (L/d)^3 m/4b \tag{5}$$

where m is the slope of the initial linear part of the bending load *vs* deflection curve, b is the width of specimen, and L/d is the supporting span to-depth ratio.

DISCUSSION OF RESULTS

Surface Characterization

The elemental oxygen-to-carbon ratios on the polyethylene fiber surfaces can be obtained from the relative areas under the O_{1s} and C_{1s} peaks of the XPS spectra, suitably corrected for relative sensitivity. The results are reported in Table II and

TABLE II
Composition of Carbon and Oxygen on the Surface of High-Modulus Polyethylene Fibers with Different Surface Treatments

Surface Condition	Carbon %	Oxygen %	O/C Ratio
Untreated	81.7	16.6	0.20
Untreated/Extracted	97.1	2.9	0.03
Plasma-Treated	84.4	19.6	0.23
Plasma-Treated/Extracted	89.7	10.3	0.11

indicate that the oxygen content of the treated fibers (19.6%) is only slightly higher than that of the untreated fiber (16.6%). After methanol extraction, however, the oxygen contents are reduced to 10.3% and 2.9%, respectively, indicating that more than half of the oxygen on the surface of the plasma-treated fibers is strongly bonded while nearly all of the oxygen on the untreated fibers is weakly physisorbed. The untreated fibers also have 1% of impurities, such as phosphorous and sodium.

Deconvolution of the C_{1s} and O_{1s} peak profiles are shown in Figures 2 and 3. In deconvoluting the original profiles into difference peaks, we adopted a Gaussian shape

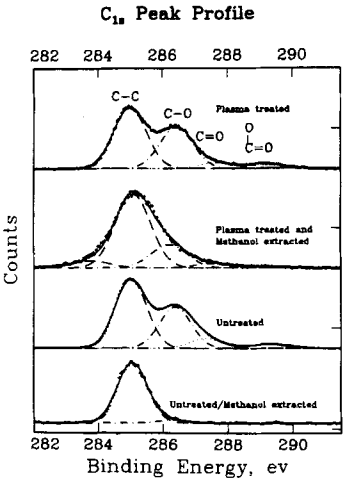

FIGURE 2 C_{1s} Spectra and their Deconvoluted Peaks for Different Chemical Groups of Carbon Elements on High-Modulus Polyethylene Fiber Surface.

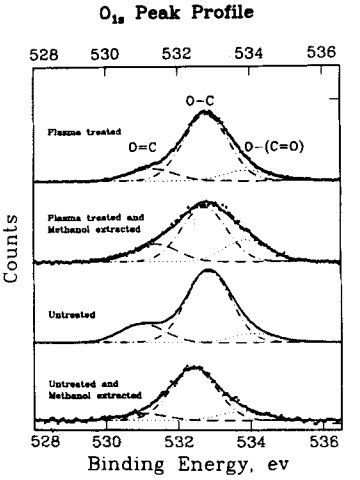

FIGURE 3 O_{1s} Spectra and their Deconvoluted Peaks for Different Chemical Groups of Oxygen Elements on High-Modulus Polyethylene Fiber Surface.

for each peak, and forced the full width at half maximum to be same for each peak. This is at best only an approximation of reality. Calculations of the chemical compositions at the surfaces of the fibers are reported in Tables III and IV. Nearly ninety percent of carbon bonds exist in the form of C—C and C—O groups, while the carbonyl-carboxylic-, and ester- containing compounds account for less than 10% of the total. The oxygen in carbonyl-, carboxylic- and ester-containing compounds accounts for about 20% of the total oxygen content on the untreated fiber surfaces and about 26% on the plasma-treated surfaces prior to extraction. The C—O could be either in the form of hydroxyl C—OH, ether C—O—C, ester C—O—C=O, or epoxide  . The fraction of hydroxyl groups present can be estimated from the XPS spectra for untreated and plasma-treated fibers after treatment with trifluoric acetic anhydride. The element ratio of F/O is 0.075 for the plasma-treated fibers and 0.030 for untreated fibers after the fibers were dried at 90°C for 30 min. Thus, oxygen in the form of C—OH constitutes only 2.5% of total oxygen for plasma-treated fibers and 1% for untreated fibers. When the same fibers were dried at 90°C for 4 hours, the F/O ratio for the plasma-treated fibers decreased to 0.030 while that for untreated fiber becomes nearly zero. It is not certain whether the decrease in fluorine content is due to the removal of physisorbed molecules or to the thermal decomposition of the tagged groups. In any case, only a small fraction of total oxygen exists in the form of the hydroxyl groups, confirming that C—O exists mostly in the form of ether and/or epoxy linkages.

Figure 4 shows DRIFT spectra for different surface conditions. Peak assignments are listed in Table V. The three forms of C—O groups, *i.e.* C—O—H, C—O—C, and C—O—C=O can be identified. However, it is difficult to obtain quantitative

TABLE III
Chemical Composition Determined from the Peak Profile of C_{1s}

Composition	C—C		C—O		C=O		O—C=O	
	E_b, ev	Content	E_b, ev	Content	E_b, ev	Content	E_b, ev	Content
Untreated	285.0	0.55	286.4	0.33	287.4	0.079	289.2	0.036
Untreated/Extracted	285.1	0.95	286.4	0.045				
Plasma-Treated	285.0	0.55	286.4	0.37	287.7	0.052	289.2	0.038
Treated/Extracted	285.1	0.64	286.2	0.21	287.6	0.042	289.0	0.018

TABLE IV
Oxygen Chemical Composition Determined from the Peak Profile of O_{1s}

Composition	O—C		O—C		O—C=O	
	E_b, ev	Content	E_b, ev	Content	E_b, ev	Content
Untreated	531.0	0.18	532.8	0.73	534.1	0.09
Untreated/Extracted	531.4	0.10	532.7	0.79	534.0	0.11
Plasma-Treated	531.3	0.14	532.8	0.74	533.9	0.12
Treated/Extracted	531.4	0.22	532.9	0.62	533.9	0.16

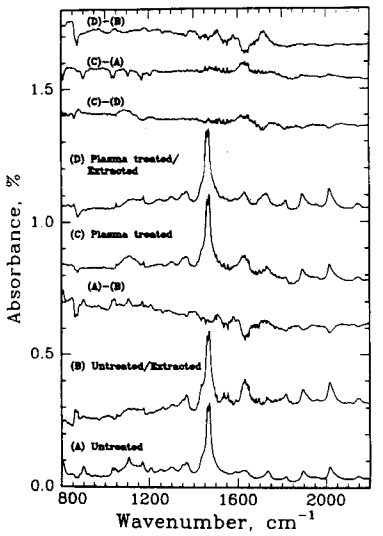

FIGURE 4 Diffuse Reflectance FT-IR (DRIFT) Spectra of High-Modulus Polyethylene Fibers.

TABLE V
Peak Assignments for IR Spectrum

Wavenumber, cm^{-1}	Structure and Vibrational Mode
900, 1106	C—O Stretching in C—OH
1040	C—O Stretching in C—O—C
1207	C—O Stretching in C—O—C=O
1375	C—H Bending in CH_3
1460	C—H Scissoring Bending in CH_2
1720	C=O Stretching
1176, 1894, 2020	C—C Stretching in Trans-ethylenic Units

information on the three groups from the spectra. The carbonyl peak at 1720 cm^{-1} can also be seen. Comparing the spectra for the untreated fibers before and after methanol extraction, we can see that the peaks associated with C—O groups and C=O groups are significantly weaker after methanol extraction. For plasma-treated fibers, the C—OH stretching band at 1106 cm^{-1} becomes much weaker after methanol extraction. The difference between the spectra of plasma-treated, unextracted and untreated, unextracted fibers, (C)—(A), indicates that change in the C=O band is negligible, but that the intensity of C—OH bands decreases slightly after plasma treatment. The difference between the spectra of the extracted plasma-treated and extracted, untreated fibers, (D)—(B), indicates that the carbonyl peak intensity is strong for the plasma-treated fibers but almost negligible for the untreated fibers.

The XPS and DRIFT results are supported by surface tension measurements, reported in Table VI. The contact angle of glycerol with the untreated fibers after methanol extraction was not measured because glycerol could not form liquid drops on

TABLE VI
Contact Angle and Surface Free Energy of High-Modulus Polyethylene Fibers

	Contact Angle, Degree		Surface Energy, mJ/m^2		
Surface Condition	Epoxy	Glycerol	γ_s	γ_s^d	γ_s^p
Plasma-Treated	18.1 ($\pm$ 3.2)	41.2 ($\pm$ 9.8)	49.4	22.8	26.6
Plasma-Treated/Extracted	23.1 ($\pm$ 6.1)	62.4 ($\pm$ 9.2)	41.9	40.4	1.4
Untreated	30.1 ($\pm$ 4.9)	72.6 ($\pm$ 1.3)	40.5	39.6	0.94
Untreated/Extracted	31.3 ($\pm$ 3.6)	/	44.0	44.0	0

the fibers. We assume that the polar component, γ_s^p, is near zero for the untreated/extracted fibers, since their oxygen content is only 2.9% as shown earlier by XPS. The dispersive component, γ_s^d, is thus assumed to be 44 mJ/m^2, compared with 35.3 mJ/m^2 for regular polyethylene. This value agrees well with that obtained by Tissington *et al.*[31] for highly-drawn polyethylene fibers. Comparing the unextracted fibers before and after plasma treatments, one finds that γ_s^p increases from 0.9 mJ/m^2 for the untreated fibers to 26.6 mJ/m^2, while γ_s^d decreases from 39.6 mJ/m^2 to 22.8 mJ/m^2, indicating that the surface chemical compositions are very different even though their oxygen contents are similar. Scanning electron micrographs of the untreated and plasma-treated surfaces show similar irregular striations and grooves, indicating that differences in surface topography probably do not contribute to differences in the surface free energies. The principal difference between the two after extraction is the presence of bound carbonyl on the plasma-treated fibers.

Mechanical Test Results

Figures 5a and 5b show the average interfacial shear strength, τ_a, and the average dynamic frictional stress, τ_{fr}, for the untreated and plasma-treated fibers before and after methanol extraction. Plasma treatment increases the interfacial shear strength, τ_a, from 2.4 $\pm$ 0.7 MPa to 6.6 $\pm$ 1.0 MPa. Similarly, τ_{fr} increases from 1.7 $\pm$ 0.2 MPa for the untreated fibers to 3.2 $\pm$ 0.7 MPa for the treated fibers. After methanol extraction, τ_a for the untreated fibers increases from 2.4 $\pm$ 0.7 MPa to 3.6 $\pm$ 0.7 MPa, a statistically-significant increase at the 95% confidence limit of a *t*-test. This result further supports the evidence of a weakly-bound physisorbed layer on the untreated fibers. Methanol has virtually no effect on τ_a of the plasma-treated surface. The plasma treatment etches the weak boundary layer and probably induces cross-linking after treatment, due to the recombination of free-radicals. Tissington *et al.*[31] found a significant gel content after plasma treatments, confirming the likelihood of cross-linking.

Figure 6 shows optical micrographs of fibers embedded in the matrix. The untreated fiber has a dark appearance in contrast to the transparent matrix background, while the treated fiber is translucent. Grubb and Li[32] also observed the same patterns for the polyethylene fibers in an epoxy resin. The dark appearance for the untreated fiber is the result of poor wetting and is caused by a gap of the order of the wavelength of light existing between the fiber and matrix. The treated fiber, on the other hand, is well wetted by the matrix, thus promoting higher normal and frictional stresses during fiber pull-out.

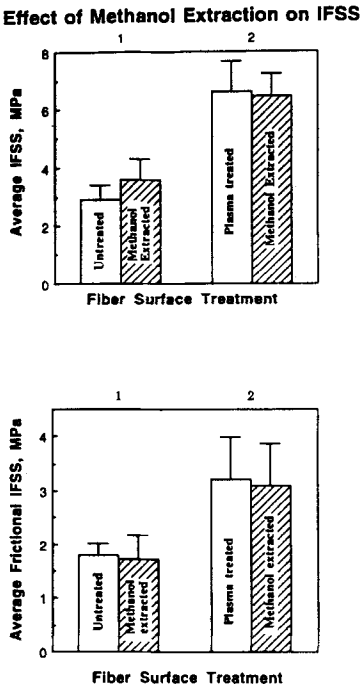

FIGURE 5 Effect of Plasma Treatment and Methanol Extraction on Interfacial Shear Strength and Dynamic Frictional Stress between High-Modulus Polyethylene Fibers and the Acrylic Resin.

The surface of an embedded, untreated fiber after pull-out has a clean appearance, featuring groove structures similar to the fiber topography before embedment. This supports the conclusion that interfacial failure occurs at a weak boundary layer. For plasma-treated fibers, resin debris is attached to some areas of the fiber surface after pull-out, indicating that interfacial failure occurs in the resin phase.

Figure 7 shows the effects of fiber sizing on the interfacial shear strengths, τ_a, before and after immersion in boiling water for 24 hours. While there are no significant changes in dry strength of the interfaces due to sizing of the plasma-treated fibers, the hydrolytic stability is improved, especially by sizing solutions containing peroxide initiator or amine accelerator. The peroxide causes the Bis-GMA monomers to polymerize on the fiber surface, while the amine accelerator forms a redox couple with the peroxides in the bulk matrix and accelerates the polymerization at the interphase. For the most part, smooth coatings are achieved with all the sizing treatments used, but with some non-uniformities that have important consequences with regard to the mode of interface failure. The sizings constitute approximately 10% by weight of the fiber, corresponding to an average thickness of about 1 μm on a 30 μm fiber. Fiber diameters varied from about 25 μm to 35 μm over the length of the fiber. The predominant mode of failure during pull-out was matrix failure near the fiber/matrix interface (Fig. 8a). In a few cases a clean fiber surface was observed upon pull-out, indicating true interface failure (Fig. 8b). In other cases, the failure surfaces showed a significant amount of

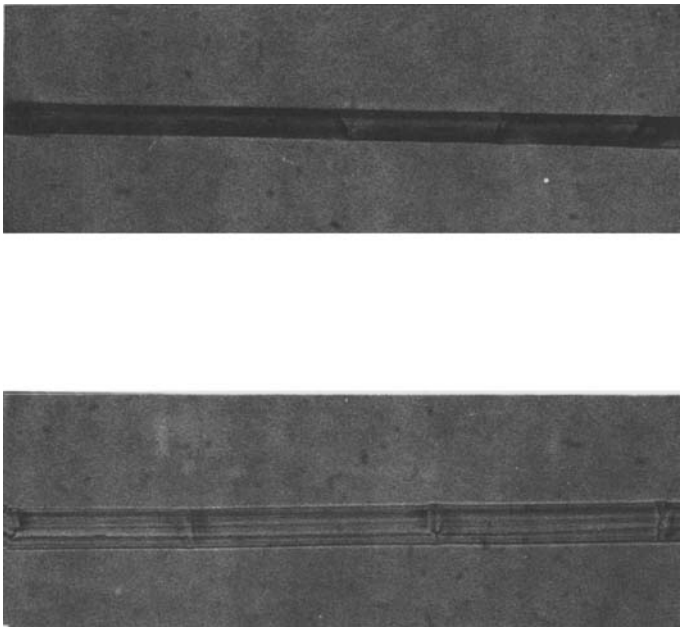

FIGURE 6 Optical Micrographs Showing (a) An Untreated and (b) a Plasma-Treated Polyethylene Fiber Embedded in the Acrylic Resin.

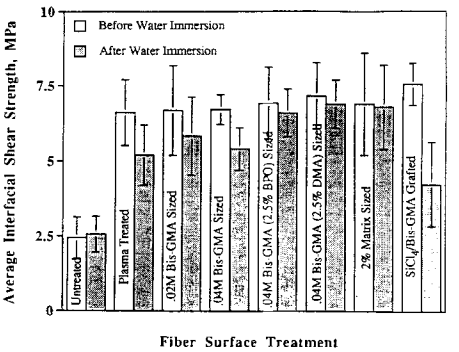

FIGURE 7 Effect of Fiber Sizings, $SiCl_4$ Treatment, and Boiling Water Immersion on the Interfacial Shear Strength between High-Modulus Polyethylene Fiber and the Acrylic Resins.

peeled fibrils from the polyethylene, indicating that the maximum attainable interfacial bond strength is limited by the shear strength of the fiber near its surface (Fig. 8c). The multiplicity of failure modes in apparently identical samples is a manifestation of the non-uniformity of the fiber surfaces and sizings. An extreme example is at kink bands, caused by compressive failure of the fiber, in which both the fiber topography and the uniformity of the sizing are disturbed. The non-uniformity of the surface then lends itself to initiation of interface failure at the worst defect along the fiber length.

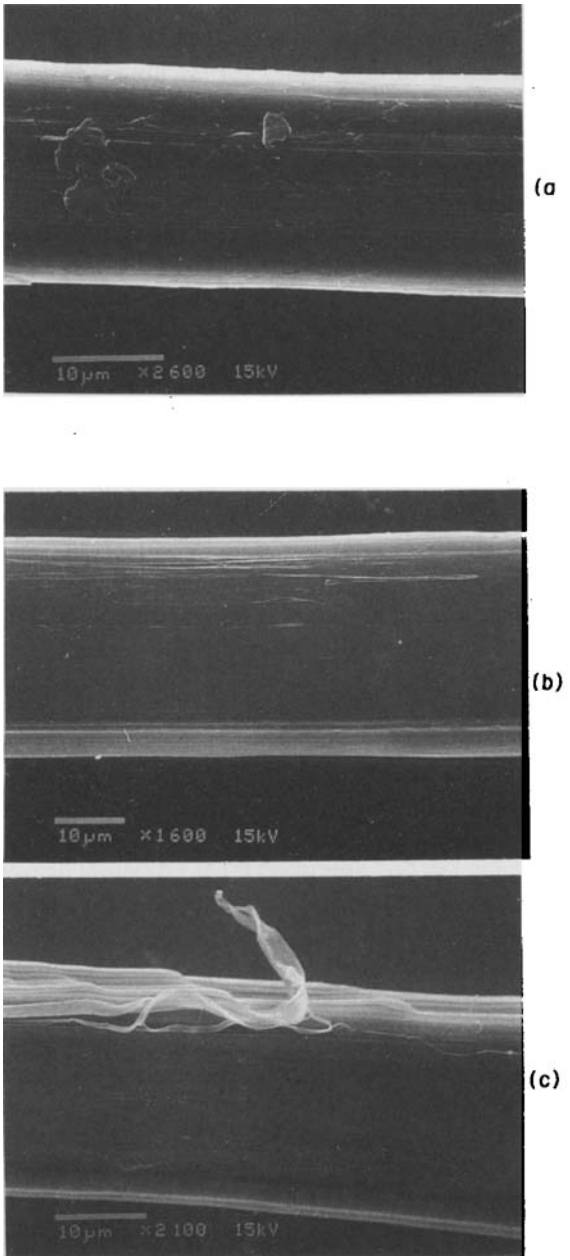

FIGURE 8 SEM Micrographs Showing Three Different Interfacial Failure Modes for Plasma-Treated Fibers Sized by 0.04M Bis-GMA with 2.5% BPO.

Figure 7 also shows the effect of $SiCl_4$ treatment and subsequent grafting of Bis-GMA on the interfacial adhesion and hydrolytic stability of the interface. The average interfacial shear strength, τ_a, increases from 6.6 ± 0.7 MPa to 7.6 ± 0.5 MPa, the largest improvement among all the surface treatments. The increase could be due to

grafting of Bis-GMA on the surfaces and/or the catalytic effect of silicon tetrachloride compounds on the polymerization of Bis-GMA. However, the interfacial shear strength after immersion in boiling water for 24 hours drops to 4.2 ± 1.5 MPa, a retention of only 54%. Siloxane linkages, such as in the silane coupling agents, have been shown to hydrolyze to form silanols, causing poor hydrolytic stability in several glass composites.[32]

The interfacial shear strength, τ_a, around 6 MPa, shown above for various surface treatments is lower than that for glass, aramid, and carbon fibers, which are of the order of 30 to 50 MPa. Even for the same fibers, different authors obtained very different values of τ_a. One major difference arises from the fact that τ_a depends on the embedded fiber length l_e. Figure 9 shows the plot of τ_a *vs* l_e for the plasma-treated fibers. When the fiber is being pulled, the shear stress is largest at the entrance of fiber to the matrix and reduces to zero at a distance away from the entrance. Using the shear-lag analysis[32] and a maximum interfacial shear strength criterion, τ_a *vs* l_e can be described using the following equation:

$$\tau_a = \tau_s \tanh(l_e/\lambda)/l_e \tag{6}$$

where τ_s is the maximum interfacial shear strength and λ is the shear-lag load transfer length. $\lambda = r_f(E_f b_i/2G_m r_f)^{1/2}$, where E_f is the Young's modulus of the fiber, G_m is the shear modulus of matrix, b_i is the effective interfacial thickness beyond which the shear stress in the matrix is negligibly small. Fitting the above equation to the experimental data, we obtain $\lambda = 0.5$ mm, and $\tau_s = 13 \pm 2$ MPa. The above relation could be used as the common base to compare the different values of τ_a obtained by different authors. An important factor in evaluating τ_a is the residual stress acting on the fibers due to the curing shrinkage of matrix, and mismatch of thermal expansion coefficient between fiber and matrix. Higher values of τ_a are obtained after correction for the residual stress.[32]

Figure 10 shows the load-deflection curves for the different fiber-reinforced composites (FRC). The calculated flexural properties of the polyethylene FRC are found to be only a fraction of those of equivalent Kevlar or E-glass FRC because of poor adhesion and low compressive strength of the polyethylene fibers. The initial bending moduli of

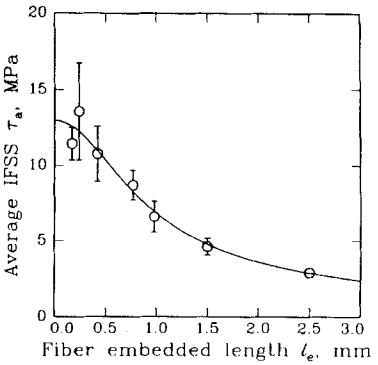

FIGURE 9 Plot of Average Interfacial Shear Strength τ_a *vs* Embedded Fiber Length, l_e.

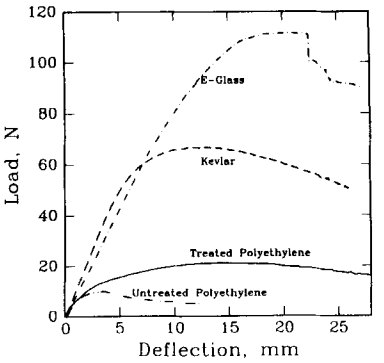

FIGURE 10 Plot of Bending Load (Normalized to fiber volume fraction = 1.0) *vs* Deflection for Different Fiber Composites.

the four composites, normalized to a fiber volume fraction of 1.0, are: 67 ± 13 GPa, 64 ± 6 GPa, 115 ± 6 GPa and 79 ± 5 GPa for the FRC with untreated polyethylene, plasma-treated polyethylene, Kevlar and E-glass fibers, respectively. The values correlate well with the tensile moduli of the fibers, independent of interface bonding. The normalized maximum flexural stresses are: 1.0 MPa, 2.1 MPa, 6.8 MPa and 11.4 MPa for the FRC with untreated polyethylene, plasma-treated polyethylene, Kevlar and E-glass fibers, respectively. The maximum flexural stresses correlate with the interfacial shear strength of the composites. While the plasma- treated polyethylene fibers generate twice the flexural load bearing capacity of the untreated polyethylene fibers, both values are much lower than those of the Kevlar and E-glass fibers. This confirms the inherent limitation of using high-modulus polyethylene fibers in applications in which the structure must bear multiaxial loads.

CONCLUSIONS

While untreated and oxygen-plasma-treated high-modulus polyethylene fibers have similar surface chemical compositions, as shown by XPS analysis, a significant amount of the oxygen-containing compounds on the plasma-treated surfaces are chemically bonded, resulting in a higher surface polarity and enhanced ability to adhere to the acrylic matrices. The average interfacial shear strength, τ_a, between the polyethylene fibers and the acrylic resins increased by a factor of 2.3 after oxygen plasma treatment. The evidence indicates that a weak boundary layer is present on the untreated fiber surfaces that results in reduced adhesion to the acrylic resins. Plasma treatment removes the weak boundary layer by chemically bonding much of the oxygen-containing compounds to the surface, thereby improving the adhesion. The hydrolytic stability of the fiber/matrix interfaces was improved by sizing the fibers with Bis-GMA prior to composite fabrication. The flexural properties of the polyethylene fiber reinforced composites were considerably poorer than those of Kevlar and E-glass fiber reinforced composites because of the relatively poor adhesion and low compressive strength of the high-modulus polyethylene fibers. Thus, the primary use of these materials in load bearing applications will be limited to those involving pure tensile

loading. They will also be useful in combination with carbon, glass or Kevlar fibers to improve the fracture toughness properties of the resulting structures.

Acknowledgements

This project was funded by U. S. Public Health Service Grant #1R01-D09126, "Fiber Reinforced Composites in Dentistry", National Institutes of Health. The authors would also like to express their gratitude to Mr. Om S. Kolluri of Plasma Sciences Inc. for providing the plasma-treated Spectra 1000 fibers.

References

1. B. Kalb and A. J. Pennings, *Polymer*, **21**, 3 (1980).
2. P. Smith, P. J. Lemstra, J. P. L. Pijpers and A. M. Kiel, *Colloid Polym. Sci.*, **259**, 1079 (1981).
3. P. J. Lemstra, R. Kirschbaum, T. Ohta and H. Yasuda, "High-Strength/High-Modulus Structures Based on Flexible Macromolecules: Gel-Spinning and Related Processes," in *Developments in Oriented Polymers-2*, I.M. Ward, Ed. (Elsevier Applied Science, New York, 1987).
4. D. C. Prevosek, "How Strong are Current High Modulus High Strength Polyethylene Fibers?," in *Polymers for Advanced Technologies*, IUPAC International Symposium, M. Lewin, Ed. (VCH Publisher, New York, 1988).
5. N. H. Ladizesky and I. M. Ward, *Compos. Sci & Tech.*, **26**, 199 (1986).
6. D. L. Gutteridge, *J. Dent.*, **20**, 50 (1992).
7. A. G. Andreopoulos, C. D. Papaspyrides and S. Tsilibounidis, *Biomater.*, **12**, 83 (1991).
8. N. H. Ladizesky, *Clin. Mater.*, **6**, 181 (1990).
9. N. H. Ladizesky, T. W. Chou and I. M. Ward, *Clin. Mater.*, **6**, 209 (1990).
10. N. H. Ladizesky and T. W. Chow, *Austra. Dental J.*, **37**, 277 (1992).
11. N. H. Ladizesky, M. K. M. Pang, T. W. Chow and I. M. Ward, *Austra. Dental J.*, **38**, 28 (1993).
12. K. W. M. Davy, S. Parker, M. Braden, I. M. Ward and H. Ladizesky, *Biomater.*, **13**, 17 (1992).
13. D. N. Hild and P. Schwartz, *J. Adhes. Sci & Tech.*, **6**, 897 (1992).
14. N. X. Nguyen, G. Riahi, G. Wood and A. Porsartip, "Optimization of Polyethylene Fiber Reinforced Composites Using a Plasma Surface Treatment," *33rd Intl. SAMPE Symposium*, pp. 1721–1729, Anaheim, CA (1988).
15. S. L. Kaplan, P. W. Rose, N. X. Nguyen and H. W. Chang," Gas Plasma Treatment of Spectra Fiber," *33rd Intl. SAMPE Symposium*, pp. 551–559, Anaheim, CA (1988).
16. M. Nardin and I. M. Ward, *Mater. Sci. & Tech.*, **3**, 814 (1987).
17. Z.-F. Li and A. N. Netravali, *J. Appl. Polym. Sci.*, **44**, 333 (1992).
18. Z.-F. Li, A. N. Netravali and W. Sachse, *J. Mater. Sci.*, **27**, 4625 (1992).
19. F. P. M. Mercx, A. Benzina, A. D. van Langeveld and P. J. Lemstra, *J. Mater. Sci.*, **28**, 753 (1993).
20. J. A. Gomez, "Oligomeric Titanates as Coupling Agents for Fiber Reinforced Composites," Ph.D. Dissertation, University of Connecticut, Storrs, CT (1989).
21. D. W. Birch, A. T. DiBenedetto and S. J. Huang, unpublished results, University of Connecticut, Storrs, CT.
22. K. Jones, "The Application of Oxazoline to Carbon Fiber Reinforced Bismaleimide Composites," Ph.D. Dissertation, University of Connecticut, Storrs, CT (1994).
23. L. J. Gerenser, J. F. Elman, M. G. Mason and J. M. Pochan, *Polymer*, **26**, 1162 (1985).
24. A. Garton, *Infrared Spectroscopy of Polymer Blends, Composites and Surfaces* (Hanser Publishers, New York, 1992).
25. B. J. Carroll, *J. Coll. Inter.* **57**, 488 (1976).
26. H. D Wagner, *J. Appl. Phys.*, **67**, 1352 (1990).
27. M. Weinberg, "Surface Energy Measurements of Graphite and Glass Filaments," in *Toughened Composites, ASTM STP 937*, N. J. Johnston, Ed. (American Society for Testing and Materials, Philadelphia, 1987), pp. 166–178.
28. S. Wu, "Surface and Interfacial Tensions of Polymers, Oligomers, Plasticizers and Organic Pigments," *Polymer Handbook*, J. Brandrup and E. H. Immergert, Eds. (John Wiley and Sons, New York, 1989).
29. Z.-F. Li and D. T. Grubb, *J. Mater. Sci.*, **29**, 189 (1994).
30. S. Gao and Y. Zeng, *J. Appl. Polym. Sci.*, **47**, 293 (1993).
31. B. Tissington, G. Pollard and I. M. Ward *Compos. Sci & Tech.*, **44**, 185 (1992).
32. D. T. Grubb and Z.-F. Li, *J. Mater. Sci.*, **29**, 203 (1994).